



HAL
open science

Finite element computation of residual stresses near holes in tempered glass plates

Fabrice Bernard, René Gy, L. Daudeville

► **To cite this version:**

Fabrice Bernard, René Gy, L. Daudeville. Finite element computation of residual stresses near holes in tempered glass plates. XIX International Congress on Glass, Society of Glass Technology, Jul 2001, Edinburgh, United Kingdom. pp.290-295. hal-02015137

HAL Id: hal-02015137

<https://hal.science/hal-02015137>

Submitted on 27 Feb 2019

HAL is a multi-disciplinary open access archive for the deposit and dissemination of scientific research documents, whether they are published or not. The documents may come from teaching and research institutions in France or abroad, or from public or private research centers.

L'archive ouverte pluridisciplinaire **HAL**, est destinée au dépôt et à la diffusion de documents scientifiques de niveau recherche, publiés ou non, émanant des établissements d'enseignement et de recherche français ou étrangers, des laboratoires publics ou privés.

Finite element computation of residual stresses near holes in tempered glass plates

F. Bernard^{1,2} R. Gy² & L. Daudeville^{3,4}

¹Laboratoire de Mécanique et Technologie, 61 av. du Pt Wilson, 94235 Cachan Cedex, France

²Saint-Gobain Recherche, 39 Quai Lucien Lefranc, BP 135, 93304 Aubervilliers Cedex, France

³Laboratoire Sols Solides Structures, Domaine Universitaire, BP 53, 38041 Grenoble Cedex 9, France

This work presents numerical results of the thermal tempering simulation by the finite element method in order to calculate residual stresses near edges of a glass plate (2D calculation) and near chamfered holes (3D calculation). During thermal tempering, glass is considered as a viscoelastic material. Narayanaswamy's model is used; it takes into account the structural relaxation phenomena. Particular difficulty is the correct modelling of heat transfers since residual stresses strongly depend on the history of temperature within the plate, close to the edges and in the vicinity of the hole. Both the forced convection due to the blowing of air and the radiative heat transfer are modelled numerically. The semi-transparency of glass in the near infrared range is considered. The convective heat transfer coefficients on the edge and hole walls are identified thanks to a specific experimental set-up and validated from simulations of heat transfer tests. The computed residual stresses are checked against photoelastic measurements.

In the design of high load bearing capacity beams made of tempered flat glass, connections cannot be avoided when long beams or inertia beams are considered. The studied technology is derived from the one used for hung glass, for façades for example. In such structural applications, glass plates are loaded through metallic dowel type joints. This metallic connector is inserted in a chamfered hole of the glass plate.

The first stage of the study is the calculation of the residual stresses in the vicinity of the chamfered hole (3D calculation). Previous studies of glass tempering have been concerned with the calculation of residual stresses in infinite plates, i.e. far away from edges and possible holes, by means of 1D modelling.⁽¹⁾ The computation of residual stresses in the vicinity of a straight edge (2D modelling) was carried out⁽²⁾ and near holes⁽³⁾ but these previous analyses were not taking into account, in an exhaustive way, the heat transfers occurring during the tempering process.

The present contribution concerns the prediction of transient and residual stresses, not only close to straight

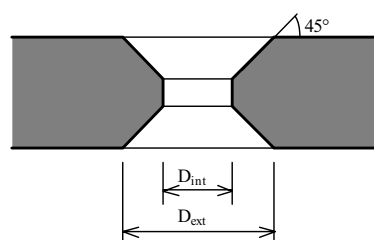


Figure 1. Chamfered holes

edges but also in the vicinity of chamfered holes of 19 mm thick glass plates. A thermomechanical calculation is carried out with the finite element method (FEM). Knowledge of both the mechanical behaviour of glass and temperature history in the whole plate during the tempering process are then necessary.

This paper focuses on the identification of the different heat exchanges. Several hole geometries are considered: large, mean and small 45° chamfers. Finally, this study allows us to determine which hole geometry obtains the best reinforcement.

Description of the holed plates

The considered glass is a 19 mm thick Planilux glass produced by Saint-Gobain. For such structural applications glass plates are loaded in their plane; that is why chamfered holes are symmetrical. The fabrication was carried out by the Saint-Gobain company. Five different geometries are studied, Figure 1 and Table 1.

Mechanical behaviour

At room temperatures glass behaves like an elastic solid whereas at high temperatures it can be considered as viscous liquid. In the transition zone, glass is a viscoelastic and thermorheologically simple material. The structural relaxation phenomenon has to be taken into account in the modelling of the quenching proc-

Table 1. Five different studied geometries

Designation	D_{int} (mm)	D_{ext} (mm)
a1	38	40
a2	54	56
b1	24	40
b2	40	56
c1	30	40

⁴ Author to whom correspondence should be addressed (e-mail: Laurent.Daudeville@hmg.inpg.fr)

ess. This mechanical behaviour was widely studied in the literature. Narayanaswamy⁽⁴⁾ proposed a model that includes both structural and viscous relaxation phenomena. Narayanaswamy's model was implemented in the software Abaqus for the present study. This model is now briefly presented.

Linear viscoelastic behaviour of glass

The temperature is first considered as constant. The viscoelastic behaviour is described in terms of stress relaxation by means of a generalised Maxwell model. The bulk part is separated from the deviational one. Relaxation shear and bulk moduli are described with instantaneous and deferred moduli and expanded into Prony's series of six terms.⁽⁵⁾

Thermorheological simplicity

The thermorheological simplicity feature consists in considering that temperature (*T*) and time (*t*) are two dependent state variables. Indeed relaxation functions have the same form for different temperatures; they are only translated along the temperature scale. Thus the knowledge of the glass behaviour at a reference temperature allows its knowledge at any other temperature by the intermediary of the reduced time (ξ).⁽⁶⁾ This one is defined thanks to the shift factor (Φ), which is the ratio of the actual viscosity (η) and the viscosity at the reference temperature (η_{ref})

$$d\xi = \Phi(T)dt \text{ and } \Phi(T) = \frac{\eta(T)}{\eta_{ref}}$$

Temperature dependence of the viscosity is assumed to follow the VFT (Vogel-Fulcher-Tamman) law.⁽⁷⁾

Structural relaxation

The structural relaxation is a direct consequence of the thermodynamic definition of glass: the structural state of glass depends on the cooling rate during thermal tempering. This phenomenon is taken into account thanks to the concept of fictive temperature (T_f) which represents the temperature of the liquid which is in the same structural state as the considered glass at temperature.⁽⁸⁾ By analogy with the viscous relaxation, a response function $M_v(\xi)$ is defined and expanded into Prony's series.⁽⁴⁾ This function allows the definition of the variation of fictive temperature with time

$$T_f(t) = T(t) - \int_0^t M_v [\xi(t) - \xi(t')] \frac{dT(t')}{dt'} dt'$$

All the temperature dependent parameters are functions of fictive temperature. All parameters of the presented model were identified by Saint-Gobain Recherche.⁽²⁾

Identification of heat transfer phenomena during tempering

In the tempering of glass, and rather in the generation of residual stresses, temperature plays a crucial role. Heat exchanges are made by conduction, thermal ra-

diation and convection. The conductive flow (Φ_c) follows the Fourier law

$$\Phi_c = -\lambda(T) \text{grad } T$$

The thermal conductivity (λ) varies linearly with temperature. Its expression is identified by Saint-Gobain Recherche (the dimensions are in $Wm^{-1}K^{-1}$).

$$\lambda = 0.975 + 8.58 \times 10^{-4} (T - 273)$$

The cooling by air casts is modelled by forced convection. Far away from edges, the forced convection is characterised by a heat transfer coefficient and by the air temperature. For the modelling of the tempering of holed plates, several coefficients are defined (in the hole, on the straight edges...).

In addition, because of the high temperature at the beginning of the tempering process, modelling of the thermal radiation is necessary.

Thermal radiation modelling

Radiation is a complex phenomenon in glass which is a semi-transparent medium since infrared waves are not stopped by the first molecular layers they meet, opposite to the other opaque materials of civil engineering: steel, concrete, timber...⁽⁹⁾

Radiation modelling for the infinite plate is done as follows. The radiative flow is split into two flows which emanate from surfaces on the one hand and from volume on the other hand. Thus surface and volume emissivities of glass plates are defined in the following way: the surface emissivity (ϵ_{surf}) is defined for the spectral field where glass is opaque, the radiative transfers take place only on the surface; the volume emissivity (ϵ_{vol}) is defined for the spectral field where glass is semi-transparent, the radiative transfers occur in all the volume of glass.

It is assumed that radiative transfers take place in a uniform way in all the volume. The surface flow is given by

$$\Phi_s = 2 \left[\epsilon_{surf}(T_s) \sigma T_s^4 - \epsilon_{surf}(T_{ext}) \sigma T_{ext}^4 \right]$$

Where T_s is the surface temperature, T_{ext} the environment temperature and s the Stefan-Boltzmann coefficient.

The factor 2 represents the heat exchanges of the two faces of the plate.

The volume flow is given by

$$\Phi_v = 2\sigma \left[\epsilon_{vol}(e, T_v) T_v^4 - \epsilon_{vol}(e, T_{ext}) T_{ext}^4 \right]$$

where T_v is the mean temperature in the thickness (e) of the glass plate.

The factor 2 is due to the heat exchanges with the two semi-spaces above and under the plate.

It is then assumed that each point of the volume only exchanges radiative energy with the outside and not with the neighbouring points within the volume. The surface and volume emissivities are numerically obtained as explained by Banner & Klarsfeld for the apparent emissivity of flat glass⁽¹⁰⁾ with the improvement here that the radiative flow is split into two parts as already explained, corresponding to the two spectral ranges where glass is opaque or semi-transparent,

for the surface or volume emissivity, respectively. The numerical results for the two emissivities are put into polynomial forms which are easy to handle with the FE code Abaqus. On each Gauss point (i), the emitted radiative flow (respectively absorbed) is calculated by multiplying the volume emissivity by (σT_i^4) (respectively σT_{ext}^4) divided by the thickness of the glass plate. On the surface the flow corresponding to the opaque spectral field, which results from a similar calculation with the surface emissivity, is added.

Questions. The two main assumptions are now discussed for the 19 mm thick glass plates: the uniform radiative exchanges in the volume and the 1D expressions of emissivities.

The insight penetration of a radiation does not pass from zero to all the volume. In fact the reduction of the radiation intensity (I) follows an exponential law

$$I = I_0 \exp(-K_\lambda x_2)$$

where K_λ is the absorption factor and x_2 the thickness coordinate.

Assuming uniform radiative exchanges in the volume is correct for thin glass plates, is it still valid for thick plates?

The emissivities are determined for infinite plates. In the vicinity of edges and holes their expressions are theoretically not the same (the problem to solve is 3D). Is it possible to use 1D expressions of emissivities kept constant in the vicinity of edges and holes?

Validation of the modelling. These two assumptions were checked thanks to experimental results. 250 mm wide, 250 mm large and 19 mm thick glass plates, perforated or not, were heated to temperatures where the thermal radiation is very present. Then they were cooled by free convection in order to give the importance to the radiation compared to the convection.

During the cooling, the plate was observed with an infrared camera. A 5 μ m filter was used in order to record the radiation emitted by the surface only because glass can be considered as opaque for this wavelength. This information allowed the determination of the surface temperature.

Residual stresses depend on the history, during the cooling, of the difference between the surface and the volume temperatures within the plate. They are measured by photoelastic methods: the surface residual stresses are obtained with the epibiascope which sends a ray of light in a parallel direction to the surface and which uses the 'mirage' effect on the tin side.⁽¹¹⁾ With conventional photoelastic analysis (transmitted light), it is possible to obtain the membrane stress (Σ) defined as

$$\Sigma = \frac{1}{e} \int_{-e/2}^{e/2} (\sigma_{33}(x_2) - \sigma_{11}(x_2)) dx_2$$

where x_2 is the thickness coordinate. This one can be neglected everywhere in the plate except near the edge and the hole where the normal stress is equal to zero.

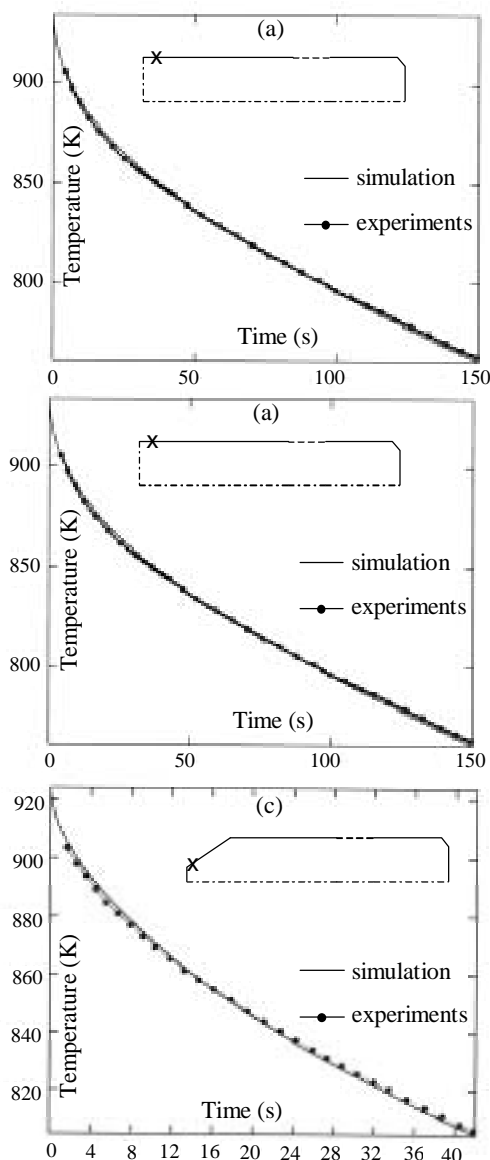


Figure 2. Comparisons experimental and calculated surface temperatures: (a) in the inner zone of the plate; (b) close to the edge; (c) on the hole chamfer

The numerical simulation of the free convection tests, taking into account the infrared radiation, allows the temperature on different points of the plate to be found (far away and in the area of edges and holes). Figure 2(a)–(c) shows the comparisons between experimental and numerical results. The good agreement, shown in Table 2, between the experimental and predicted values of residual stresses assures the right calculated temperatures on every point within the plate. The results obtained far from the edges and the hole

Table 2. Comparisons between experimental and calculated residual stresses in different locations of the plate (Figure 2)

	Experimental (MPa)	Calculated (MPa)
Inner surface stress far away from the hole and the edge (a)	-67.4	-69.4
Membrane stress close to the edge (b)	-94.4	-91.8
Surface stress close to the hole (c)	-73.2	-74.4



Figure 3. Holed model b2

assure that the radiative transfers can be considered as uniform in all the volume, whereas the results near the edges and in the vicinity of hole validate the 1D expressions of the emissivities in this 3D area.

The model of heat transfer per radiation is then pertinent.

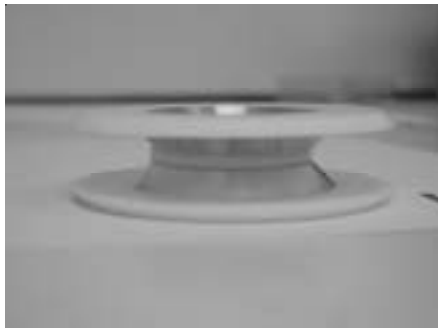


Figure 4. Zoom on the constituents of the chamfered hole

Identification of forced convection coefficients

The convection coefficients in the different area of perforated plates are identified using a hollow aluminium model representative of the external surface of a 400×400×19 mm³ glass plate. Figures 3 and 4 show this model. Each aluminium element is isolated from the others thanks to PTFE washers. All of them are instrumented with thermocouples as is described in Figure 5. The thermocouples are distributed everywhere on the perforated plate.

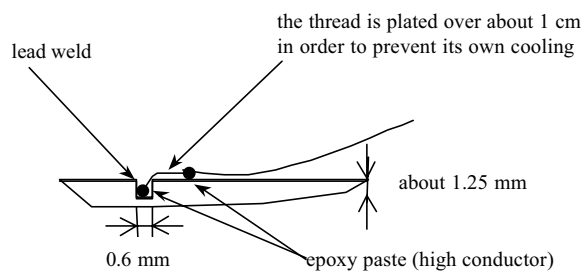


Figure 5. Description of the thermocouples

Table 3. Different identified forced convection coefficients (W/m²K)

h	Plate faces		Chamfered zones			Cylindrical zones		Edges
	Far away from the hole	Close to the hole	b1	b2	c1	a1	a2	
	77	72	74	78	75	58	61	62

Table 4. Comparisons between predicted and measured surface stresses (MPa)

Measured with the epibiascope	Simulation
-147	-144

The model is then submitted to real conditions of tempering but is heated to a temperature such as the radiation is negligible. The temperature is recorded thanks to the thermocouples during the cooling process.

Neglecting the conduction term in the heat equation (the aluminium conductivity is very high, so the temperature gradient through the thickness is low), the temperature is given by Ref. 12

$$d\rho c_p \frac{dT}{dt} = h(T_{air} - T)$$

where *d* is the thickness of the plate, ρc_p the thermal capacity, *h* the convection coefficient and *T*_{air} the air temperature.

Assuming that *h* and *c_p* are constant, the previous equation gives the time dependence of temperature

$$T = (T_0 - T_{air}) \exp\left(-\frac{ht}{d\rho c_p}\right) + T_{air}$$

where *T*₀ is the initial temperature. The actual forced convection coefficients on different locations where the temperature is recorded is then given by

$$h = -\frac{1}{t} d\rho c_p \ln\left(\frac{T - T_{air}}{T_0 - T_{air}}\right)$$

All identified coefficients are given in Table 3.

Calculation of residual stresses

Validation

All the heat transfers are now identified. The accurate prediction of the residual stresses due to the tempering of thick perforated glass plates is then possible.

The two emissivities model is used to account the thermal radiation. The convection coefficients are those identified with the previous experiments. The initial temperature is given by the manufacturer (630°C). The

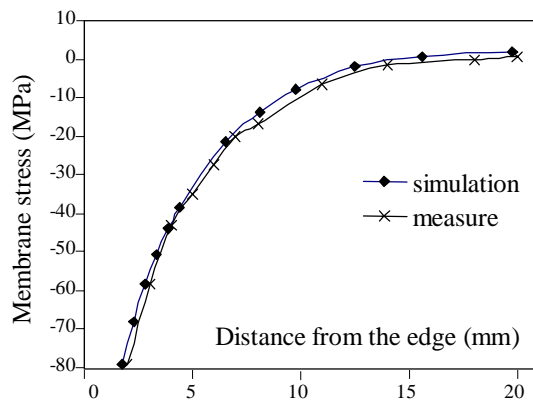


Figure 6. Comparisons between predicted and measured membrane stresses close to the edge (the measures started from the chamfer)

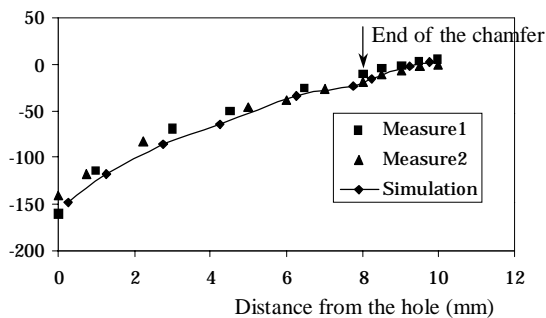


Figure 7. Comparisons between predicted and measured membrane stresses in the vicinity of the hole (for a hole with a large chamfer)

air temperature was measured during the previous experiments (20°C). The finite element modelling of the thermal process is assumed to be axisymmetric since the thermocouples reveal the cooling symmetries between all the points of the hollow model.

50 tempered perforated glass plates were analysed. Their residual stresses were determined in order to check the FE simulation. The comparisons are made on two different points: the surface stresses far away from the hole and the edge; they were obtained thanks to the epibiascope; the membrane stresses in the vicinity of the hole and the edge were measured with the transmitted light (the hole is full of a liquid of same refraction index as glass).

Table 5. Summary table of the predicted results

Type	Surface stress σ_{33} (MPa)			Membrane stress (for $x_1=0$) (MPa)	Neutral line position (mm)	Compression thickness (mm)
	Min.	Average	Max.			
a1	-106.1	-123	-149.8	-119.6	5.38	3.00
a2	-114.6	-127.7	-149.7	-125.1	6.08	3.35
b1	-133.1	-143.8	-157.6	-155.2	8.94	3.70
b2	-136.6	-147.9	-157.7	-155.6	9.49	4.00
c1	-119.2	-133.1	-142.4	-131.4	6.50	3.64

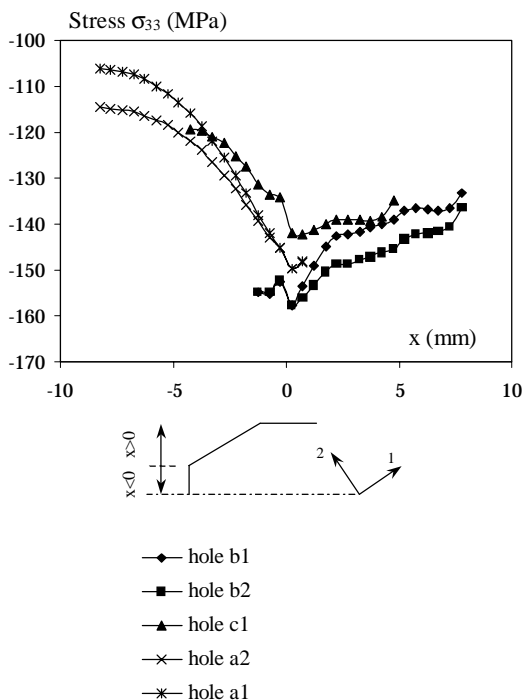


Figure 8. Predicted surface stress σ_{33} for each kind of hole geometry

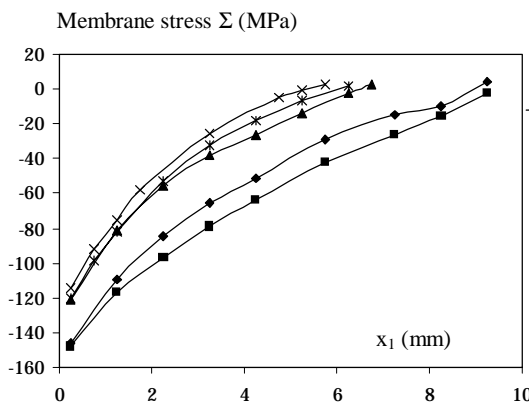


Figure 9. Predicted membrane stress

$$\Sigma = \frac{1}{e} \int_{-e/2}^{e/2} (\sigma_{33}(x_2) - \sigma_{11}(x_2)) dx_2$$

for each kind of geometry

An estimation of these stresses lower than 10 % with a maximum of 10 MPa is then obtained.

Table 4 and Figures 6 and 7 show good agreement between calculated and measured stresses on the samples. It concludes the validation of the thermal tempering modelling.

This simulation can now be used in order to identify the hole geometry which obtains the best reinforcement after tempering.

Application of the simulation

The considered criteria for the analysis of the reinforcement are: the surface tangential stresses in the hole; the membrane stresses in the vicinity of the hole; the neutral line: beyond this line a zone of integrated tension occurs, that may weaken the hole; the compression thickness in the vicinity of the hole.

All the comparisons for the five different hole geometries of this study are grouped together in Figure 8, 9 and in Table 5. These results allow the conclusion that the best reinforcement is obtained for the two holes with large chamfers. The tempering process is the most effective for these kinds of geometry.

Conclusion

The determination of the load bearing capacity of joints in tempered glass structures passes first by the

finite element computation of residual stresses near holes. In this analysis the heat transfers occurring during tempering play a crucial role, in particular thermal radiation and forced convection. The thermal radiation is taken into account with the two emissivities method. The pertinence of this modelling for structural glass is experimentally proved. The actual forced convection coefficients are identified thanks to a hollow aluminium model submitted to real conditions of tempering. These coefficients are different far away and in the vicinity of edges and hole. The identification of these heat exchanges, with the use of the Narayanaswamy's mechanical behaviour model, allows us to conclude that the tempering process is the most effective for holes with large chamfers.

References

1. Narayanaswamy, O. S. & Gardon, R. Calculation of residual stresses in glass. *J. Am. Ceram. Soc.*, 1969, **52** (10), 554–8.
2. Carré, H. & Daudeville, L. Load bearing capacity of tempered structural glass. *ASCE J. Eng. Mech.*, 1999, **125** (8), 914–21.
3. Laufs, W. & Sedlacek, G. Stress distribution in thermally tempered glass panes near the edges, corners and holes. Part 1. Temperature distributions during the tempering process of glass panes. *Glass Sci. Technol.*, 1999, **72** (1), 1–14.
4. Narayanaswamy, O. S. A model of structural relaxation in glass. *J. Am. Ceram. Soc.*, 1971, **54** (10), 491–8.
5. Gy, R., Duffrene, L. & Labrot, M. New insights into the viscoelasticity of glass. *J. Non-Cryst. Solids*, 1994, **175**, 103–17.
6. Schwarzl, F. & Staverman, A.J. Time-temperature dependence of linear viscoelastic behavior. *J. Appl. Phys.*, 1952, **23** (8), 838–43.
7. Duffrene L. *PhD Thesis*. Ecole Nationale Supérieure des Mines de Paris, 1994.
8. Tool, A. Q. Relation between inelastic deformability and thermal expansion of glass in its annealing range. *J. Am. Ceram. Soc.*, 1946, **29** (9), 240–53.
9. Banner, D. *PhD Thesis*, Ecole Centrale de Paris. 1990.
10. Banner, D. & Klarsfeld, S. Influence of composition upon the apparent conductivity and emissivity of glass as a function of thickness and temperature. *Thermal conductivity 21*. 1990. Edited by C. J. Cremers & H. A. Fine. Plenum Press, New York.
11. Aben, H. & Guillemet, C. *Photoelasticity of glass*. 1993. Springer-Verlag, Berlin.
12. Holman, J. P. *Heat transfer*. 7th edition. 1992. McGraw-Hill, New York.